Antisense oligonucleotide strategies to increase progranulin levels for frontotemporal dementia

Geetika Aggarwal[a,b,c,1], Subhashis Banerjee[a,b,c,1], Spencer A. Jones[a,b,c], Denise M. Smith[a,b,c], Yousri Benchaar[d], Jasmine Bélanger[d], Myriam Sévigny[d], Monica Pavlack[b,c], Michael L. Niehoff[a,e], Ian Mitchelle S. de Vera[b,c], Terri L. Petkau[f], Blair R. Leavitt[f,g,h], Karen Ling[i], Paymaan Jafar-Nejad[i], Frank Rigo[i], John E. Morley[a], Susan A. Farr[a,b,c,e], Paul A. Dutchak[d], Chantelle F. Sephton[d], Andrew D. Nguyen[a,b,c,2]

[a]Division of Geriatric Medicine, Department of Internal Medicine, Saint Louis University School of Medicine, St. Louis, MO 63104
[b]Department of Pharmacology and Physiology, Saint Louis University School of Medicine, St. Louis, MO 63014
[c]Henry and Amelia Nasrallah Center for Neuroscience, Saint Louis University, St. Louis, MO 63104
[d]Department of Psychiatry and Neuroscience, CERVO Brain Research Centre, Laval University, Quebec City, Quebec, Canada
[e]Veterans Affairs Medical Center, St. Louis, MO 63106
[f]Centre for Molecular Medicine & Therapeutics, Department of Medical Genetics, University of British Columbia, B.C. Children's Hospital, Vancouver, BC, Canada
[g]Division of Neurology, Department of Medicine, University of British Columbia Hospital, Vancouver, BC, Canada
[h]Center for Brain Health, University of British Columbia, Vancouver, BC, Canada
[i]Ionis Pharmaceuticals, Carlsbad, CA 92010

[1]G.A. and S.B. contributed equally to this work.
[2]Corresponding author: Andrew D. Nguyen, Division of Geriatric Medicine, Department of Internal Medicine, Saint Louis University School of Medicine, 1402 S. Grand Blvd, St. Louis, MO 63104. Phone: 314-977-4036. Email: andy.d.nguyen@health.slu.edu

Keywords: Progranulin, frontotemporal dementia, antisense oligonucleotides, microRNA, haploinsufficiency

Abstract

GRN mutations cause frontotemporal dementia (FTD) due to haploinsufficiency of progranulin. Several microRNAs, including miR-29b, negatively regulate progranulin protein levels. Antisense oligonucleotides (ASOs) are emerging as a promising therapeutic modality for neurological diseases, but ASO-based strategies for increasing target protein levels are limited. Here, we tested if ASOs can increase progranulin levels by sterically blocking the miR-29b binding site in the 3' UTR of the human *GRN* mRNA. We found 16 ASOs that increase progranulin protein levels in a dose-dependent manner in neuroglioma cells. A subset of these ASOs also increased progranulin levels in iPSC-derived neurons and in a humanized *GRN* mouse model. Ribosomal profiling experiments revealed that the ASOs increase the rate of progranulin translation. Consistent with this, ASO treatment increased levels of newly synthesized progranulin protein. In FRET-based assays, the ASOs effectively competed miR-29b from binding to the *GRN* 3' UTR RNA. Together, our results demonstrate that ASOs can be used to effectively increase target protein levels by partially blocking miR binding sites. This ASO strategy may be therapeutically feasible for progranulin-deficient FTD as well as other conditions of haploinsufficiency.

Introduction

Progranulin is a lysosomal and secreted protein with pleiotropic effects, including promoting neuronal survival, neurite outgrowth, wound healing, tumor cell growth, and modulating inflammation (1, 2). Haploinsufficiency of progranulin causes frontotemporal dementia (FTD) (3, 4), and thus increasing progranulin levels is a clear therapeutic goal (5, 6). Gene therapy studies in mice provide proof of concept that restoring progranulin levels in heterozygous *Grn* mice improves FTD-associated neuropathology and behavioral deficits (7). Current therapeutic efforts are focused on small molecules that increase progranulin expression (8-11), gene therapies (7, 12), monoclonal antibodies that modulate progranulin trafficking (13), and protein replacement (14). However, there are currently no approved therapies for progranulin-deficient FTD.

Antisense oligonucleotides (ASOs), short synthetic oligonucleotides used to modulate target RNAs, are emerging as a promising therapeutic modality for neurological diseases (15, 16). The most commonly used ASO strategies involve RNase H1-mediated degradation of the target mRNA and modulation of splicing of the target mRNA (15). ASO-based strategies for increasing target protein levels are still relatively limited. Several strategies have been reported, including targeting upstream ORFs (uORFs) and regulatory elements in the 5' UTR (17, 18). However, these approaches are limited by the fact that not all genes possess uORFs and/or 5' regulatory elements.

MicroRNAs (miRs) have been estimated to regulate more than 60% of all human proteins (19). These miRs typically bind to the 3' UTR of target mRNAs and decrease protein levels through translational repression or mRNA decay (20, 21). For progranulin, three miRs have been reported to negatively regulate progranulin protein levels: miR-29b, miR-107, and miR-659 (22-

26). The binding sites of miR-29b and miR-659 have been mapped to the *GRN* 3' UTR (22-25). Notably, the miR-659 binding site overlaps with the rs5848 SNP (24), which is a risk factor for FTD (24) and Alzheimer's disease (27, 28). Individuals with the TT genotype (minor allele) at rs5848 have ~30% decreased progranulin protein levels in brain tissue and in CSF (24, 29), suggesting that miR-mediated modulation of progranulin levels contributes to risk of these forms of dementia. Thus, these miRs present as potential targets for increasing progranulin protein levels.

In the current study, we tested a therapeutic strategy for increasing progranulin protein levels by using ASOs to target the miR-29b binding site in the human *GRN* mRNA. We show that these ASOs effectively increase progranulin protein levels in cultured cells, iPSC-derived neurons, and in mouse brains. Additionally, we determined the mechanism of action is that these ASOs displace miR-29b from its binding site and thereby de-repress translation, resulting in increased progranulin protein levels.

Results

ASOs targeting the miR-29b binding site increase progranulin protein levels

Previous studies have reported that miR-29b inhibition increases progranulin protein levels in cells (22, 23). We confirmed that treatment with a broad miR-29b inhibitor increases progranulin protein levels in a dose-dependent manner (Fig. 1A) in H4 human neuroglioma cells, which have moderate expression of miR-29b (Fig. 1B). Data from the Human miRNA Tissue Atlas (30) show that miR-29b is expressed in the human brain (Fig. 1C).

We next sought to test if ASOs targeting the miR-29b binding site (22, 23) can increase progranulin protein levels. To this end, we designed a panel of 18-mer ASOs with 2'-*O*-methoxyethyl (MOE) ribose and phosphorothioate backbone modifications that span the entire miR-29b binding site with single nucleotide resolution (Fig. 2A). Our initial ELISA-based screening at 5 μM in H4 cells identified 11 ASOs that increased progranulin protein levels by >15% (Fig. 2B). We subsequently validated these 11 ASOs (M1, M2, M3, M5, M6, M10, M11, M31, M36, M38, M39) and identified 5 additional ASOs (M4, M25, M28, M29, M40) that increased progranulin protein levels at 10 μM, as determined by western blot (Fig. 2C). Because progranulin is also secreted from cells, we tested if the ASOs similarly increase levels of progranulin in the conditioned media. We found that ASOs that increased cellular progranulin levels also increased secreted progranulin levels (Fig. 2D), suggesting that the observed increases in cellular progranulin levels are not due to altered trafficking or secretion.

We then carried out time course and dose curve experiments for selected ASOs in H4 cells. Time course studies revealed that increased progranulin levels are detectable within 1–2 h of ASO treatment for ASOs M6 and M10, and by 8 h for ASO M36 (Fig. 3A). Dose curve experiments showed that the ASOs exhibit dose-dependent effects with EC_{50} values in the range of 1–8 μM (Fig. 3B). These ASOs exhibited no detectable toxicity in H4 cells, as determined by MTT assays (Fig. S1).

We next tested selected ASOs in iPSC-derived cortical neurons and found that these ASOs similarly increased progranulin protein levels in a dose-dependent manner (Fig. 4A). To test the ASOs *in vivo*, we used a recently developed humanized *GRN* mouse model (31); intra-striatal injection of a miR-29b inhibitor was previously shown to increase progranulin protein levels in the brains of these mice (31). At three weeks following intracerebroventricular (ICV) administration of 500 µg ASO (32), we observed increased human progranulin protein by ELISA in the cortex of mice that received ASO M5 (Fig. 4B). Progranulin levels were increased by 53% and 55% in male and female mice, respectively, compared to mice of the same sex that received the scrambled control ASO. By western blot, we also observed increased human progranulin levels in the thalamus and hippocampus of male mice that received ASO M5 (Fig. 4C). Together, these results demonstrate that ASOs targeting the miR-29b binding site can increase human progranulin protein levels in cultured cells, neurons, and *in vivo*.

ASOs targeting the miR-29b binding site increase translation of progranulin

Despite increasing progranulin protein levels, most of the ASOs did not increase *GRN* mRNA levels in H4 cells (Fig. 5A), suggesting that the ASOs increase the rate of progranulin translation. This would be consistent with the canonical effects of translational repression by many miRs (20, 21). To formally test this, we performed ribosomal profiling experiments to assess the amount of ribosome-bound *GRN* mRNA, which reflects its rate of translation. We found that cells treated with ASOs M10 and M36 had marked enrichment of *GRN* mRNA in the heavy polyribosome fractions (11–16), compared to cells treated with a scrambled control ASO (Fig. 5B), strongly suggesting that these ASOs increase the rate of progranulin translation. To determine if the ASOs increase the amount of newly synthesized progranulin protein, we used the methionine analog azidohomoalanine (AHA) to label nascent proteins. Following immunoprecipitation of progranulin, western blots using fluorescently labeled-streptavidin confirmed that ASOs M5, M10, and M36 increase synthesis of progranulin protein (Fig. 5C).

We next tested if the ASOs act through miR-29b by using a miR-29b inhibitor. The experiments of Fig. 6A demonstrate that ASOs M5 and M10 increased progranulin levels similarly to the miR-29b inhibitor and importantly that the miR-29b inhibitor abrogated any further effects of the ASOs on progranulin levels, strongly suggesting that the ASOs block miR-29b's effect on progranulin. Lastly, we performed a FRET-based assay to test if the ASOs compete for binding of miR-29b to a partial *GRN* 3' UTR RNA containing the miR-29b binding site *in vitro*. We found that ASOs M29, M31, and M36 were able to effectively compete off miR-29b binding (Fig. 6B), with IC_{50} values in the range of 0.4–0.8 µM. The scrambled control ASO and several ASOs which do not overlap with the binding site (i.e., M2 and M5) were unable to displace miR-29b; it is possible the partial *GRN* 3' UTR RNA used in this assay does not completely recapitulate aspects of the full length *GRN* mRNA, such as secondary structure. Nonetheless, these ASOs increase translation of progranulin protein in intact cells in a miR-29b-dependent manner (Fig. 5B–C and Fig. 6A). Together, these studies establish the mechanism of action is that these ASOs displace miR-29b from its binding site and thereby de-repress translation, resulting in increased synthesis of progranulin protein.

ASOs targeting nonsense-mediated mRNA decay of the mutant Grn mRNA

In an independent ASO strategy, we previously reported that ASOs targeting nonsense-mediated mRNA decay (NMD) of the *Grn*^{R493X} mutant mRNA increase progranulin mRNA and protein levels in mouse fibroblast cells (33). Specifically, these ASOs target the exon junction complex at the 3' end of exon 12 of the mouse *Grn* mRNA (where the R493X mutation is located) to prevent binding of NMD proteins, and these ASOs thereby enable the *Grn*^{R493X} mutant mRNA to escape NMD-mediated degradation. Here, we also report *in vivo* testing of these 8 NMD-targeting *Grn* ASOs in the *Grn*^{R493X} knock-in mouse model (33). In contrast to our findings in cells, we failed to detect any significant increase in *Grn* mRNA levels in the cortex or thalamus of *Grn*$^{R493X/R493X}$ mice at 2–3 weeks following ICV administration of 200–500 µg ASO (Fig. S2A). As a positive control, we administered a validated *Malat1*-targeting ASO that is designed to decrease *Malat1* mRNA levels (32). As expected, we observed decreased *Malat1* mRNA in both the cortex and thalamus (Fig. S2B). With the NMD-targeting *Grn* ASOs, we also did not detect any increase in progranulin protein in the cortex (Fig. S3). Immunofluorescence staining confirmed broad distribution of the ASO throughout the brain in these studies (Fig. S4). Lastly, we attempted intraperitoneal (IP) administration and found these ASOs also failed to increase *Grn* mRNA levels in the livers and spleens of *Grn*$^{R493X/R493X}$ mice (Fig. S5A). As a control, the *Malat1*-targeting ASO strongly decreased *Malat1* mRNA in the livers and spleens (Fig. S5B). Together, these results demonstrate that the ASOs targeting NMD of the *Grn*^{R493X} mRNA failed to increase progranulin levels *in vivo*, despite showing efficacy in cells (Fig. S6) (33).

Discussion

In the current study, we show that ASOs targeting the miR-29b binding site can increase human progranulin protein levels in cultured cells, in iPSC-derived neurons, and in the brains of humanized *GRN* mice. In cells, the ASO effects are dose dependent and are detectable within several hours. Our mechanistic studies revealed that the ASOs act through miR-29b, compete for miR-29b binding, increase the rate of progranulin translation, and increase the amount of newly synthesized progranulin protein. To our knowledge, this is the first in-depth characterization of using ASOs to increase translation of a target protein by sterically blocking a miR binding site. Two previous studies used oligonucleotides to block miR binding sites (34, 35), but these reports lacked details about the targeting strategy and the mechanism of action. Together, our studies establish the mechanism of action is that these ASOs displace miR-29b from its binding site and thereby de-repress translation, resulting in increased progranulin protein levels.

While the current study focuses on ASOs that target the miR-29b binding site, we have also tested a smaller panel of ASOs targeting the miR-659 binding site (24, 25) in the *GRN* 3' UTR (see Fig. 2A) and identified ASOs that similarly increase progranulin protein levels (Fig. S7). Our results suggest that this ASO strategy may be broadly applicable for pharmacologically increasing levels of target proteins and could be particularly useful for development of ASO-based therapies for diseases of haploinsufficiency.

It is unclear why the ASOs targeting NMD-mediated degradation of the *Grn*^{R493X} mutant mRNA failed to increase progranulin levels *in vivo*. It is possible that these results are owing to the inherently low success rate of CNS-targeting ASOs when moving from cells to animal models. Nonetheless, it should be noted that our ASO strategy targeting the miR-29b binding site has a major advantage over the strategy targeting NMD: the miR-targeting strategy is agnostic to the specific disease mutation and could be used in the context of any of the more than 70 FTD-associated *GRN* mutations that have been identified (36). On the other hand, the NMD-targeting strategy would require development of patient-specific ASOs to target the particular exon harboring the nonsense *GRN* mutation. Overall, ASOs are proving to be a promising therapeutic modality for CNS diseases, as ASOs are versatile modulators of endogenous RNAs, well tolerated in humans, and stable in the CNS with long lasting effects (15, 16). Future studies will focus on testing if these ASOs can delay or prevent FTD-associated neuropathology and behavioral deficits in mouse models.

Materials and Methods

ASOs. ASOs used in these studies were 18-mer ASOs uniformly modified with 2'-*O*-methoxyethyl (MOE) sugars with a phosphorothioate backbone, with the following exceptions: ASOs used in the experiment shown in Fig. S7 were modified with 2'-*O*-methyl sugars with a full phosphorothioate backbone, and ASOs M2, M5, M6, and M36 in Fig. 4B–C were modified with MOE with a mixed phosphorothioate backbone. ASOs used for in vitro and cell-based studies were dissolved in water and stored at -20 °C. For *in vivo* studies, lyophilized ASOs were dissolved in sterile PBS without calcium or magnesium (Gibco, 14190-250) and sterilized by passing through a 0.2 µm filter. The miR-29b inhibitor is a 23-mer ASO containing uniform 2'-MOE sugar and phosphorothioate backbone modifications.

Cell culture. H4 human neuroglioma cells were obtained from ATCC (HTB-148) and cultured in DMEM (Dulbecco's Modified Eagle Medium, high-glucose) (Gibco, 11995-073) supplemented with 10% fetal bovine serum (FBS) (Gibco, 26140-095), 10 U/ml penicillin, and 10 µg/ml of streptomycin. For typical ASO treatments, cells were plated in 6-well or 12-well plates, and then treated with ASOs as indicated on the following day. Human iPSCs harboring doxycycline-responsive Neurogenin-2 (NGN2) expression for differentiation into i3 cortical neurons were kindly provided by Michael Ward. Cells were grown and differentiated as described (37). After 2 weeks of differentiation, i3 neurons were treated with ASOs for 3–4 days. *Grn*^{R493X} MEF cells were cultured and transfected as previously described (33). All cells were maintained at 37 °C and 5% CO_2.

ELISA and immunoblot analysis. For progranulin measurements, cells were rinsed with PBS and then lysed in RIPA buffer containing protease inhibitors (Roche, cOmplete Mini EDTA-free Protease Inhibitor Cocktail). Cleared lysates were transferred to new tubes, and protein concentrations were determined using the Bio-Rad DC Protein Assay Kit II. For ELISA, progranulin concentrations were determined in duplicate using 10–15 µl of lysates per well (typically 8–20 µg of total protein per well) using a sandwich ELISA assay (R&D Systems, DPGRN0). For experiments analyzing secreted progranulin, conditioned media was collected

and cleared at 10,000 x g for 10 min at 4° C. For western blot analysis, sample buffer was added to the lysates or conditioned media, and the samples were heated at 95 °C for 10 min. Equal amounts of protein lysates (10–20 µg) or equal volumes of conditioned media (10–20 µl) were separated on SDS–PAGE gels. Proteins were transferred to nitrocellulose membranes using the Bio-Rad Turbo-Blot transfer system. After blocking and antibody incubations, membranes were incubated with SuperSignal West Pico or Femto enhanced chemiluminescent HRP substrate (ThermoFisher) and visualized using a Chemi-Doc system (Bio-Rad). Primary antibodies used for immunoblot analysis include: an anti-human progranulin linker 5 polyclonal antibody #614 that recognizes an epitope between amino acids 497–515 (38), an anti-human vinculin monoclonal antibody (Cell Signaling Technology, 13901), and anti-mouse progranulin polyclonal antibody (R&D Systems, AF2557), and an anti-α-tubulin monoclonal antibody (Sigma, T9026). The HRP-conjugated secondary antibodies used were goat anti-rabbit IgG (H+L) (Jackson Immuno Research Labs, 111-035-144), donkey anti-mouse IgG (H+L) (Jackson Immuno Research Labs, 715035150), and donkey anti-sheep IgG (H+L) (Jackson Immuno Research Labs, 713035147).

RNA analysis. Total RNA was isolated from cultured cells using the RNeasy Mini kit (Qiagen, 74106) with on-column DNase digestion (Qiagen, 79256). RNA was reverse-transcribed to obtain cDNA using the iScript cDNA synthesis kit (Bio-Rad, 1708891), and qPCR was performed using PowerUp SYBR Green Master Mix (ThermoFisher, A25777) with a Bio-Rad CFX384 Real-Time System. Primers sequences were as follows: human CYCLO-F, GGAGATGGCACAGGAGGAAA; human CYCLO-R, CCGTAGTGCTTCAGTTTGAAGTTCT; human GRN-F, AGGAGAACGCTACCACGGA; human GRN-R, GGCAGCAGGTATAGCCATCTG; mouse 36B4-F, CACTGGTCTAGGACCCGAGAAG; mouse 36B4-R, GGTGCCTCTGAAGATTTTCG; mouse Grn-F, TGGTTCACACACGATGCGTTTCAC; and mouse Grn-R, AAAGGCAAAGACACTGCCCTGTTG. Results for qPCR were normalized to the housekeeping genes CYCLO (human) or 36B4 (mouse), and evaluated by the comparative C_T method. For RNA-seq analysis of miR levels, the small RNA fraction was isolated from triplicate 100-mm dishes of H4 cells using the mirVana miRNA Isolation Kit (Invitrogen, AM1561). Libraries were constructed using the Ion Total RNA-Seq Kit v2 (Life Technologies, 4475936) and sequenced on an Ion Torrent Proton at the Saint Louis University Genomics Core Facility. Reads were aligned to the human genome hg19 assembly, and data are presented as total normalized nucleotide coverage per miRNA. Data on miR expression levels in human tissues was from the Human miRNA Tissue Atlas (30).

Polysome profiling. H4 cells were cultured in 100-mm dishes and treated with 5 µM ASOs for 22 h. Five minutes prior to collecting cells, cycloheximide (CHX) was added to the cell culture media at a final concentration of 0.1 mg/ml. Cells were rinsed with ice-cold PBS, and then lysed in Polysome Lysis Buffer containing 20 mM Tris-HCl pH 7.4, 100 mM KCl, 5 mM $MgCl_2$, 1% NP-40, 0.1 mg/ml CHX, 1 mM DTT, 0.02 U/ml SUPERase In RNase Inhibitor (Invitorgen, AM2694), protease inhibitors (Roche, cOmplete Mini EDTA-free Protease Inhibitor Cocktail), and phosphatase inhibitors (Roche, PhosSTOP) in nuclease-free water (Invitrogen, AM9937). Lysates were centrifuged (10,000 x g, 10 min, 4 °C), and the supernatant fractions were collected. Protein determination was performed using the Bio-Rad DC Protein Assay Kit II, and 1.35 mg per sample was loaded on a 15% to 45% sucrose density gradient (w/w sucrose, 20

mM Tris-HCl pH 7.4, 100 mM KCl, 5 mM $MgCl_2$, Ultrapure water). Samples were centrifuged for 2 h at 210,200 x g at 4 °C in a SW41 Ti rotor. Polysome profiling was performed using a BR-188 density gradient fractionation system (Brandel) (sensitivity setting of 1, baseline setting of 20, and flow rate of 1.5 ml/min) with upward displacement and continuous monitoring at 254 nm using a UA-6 detector. Polyribosome (13 fractions) and monosome (3 fractions) fractions were collected in a volume of 600 µl, and the fractions were separated in two tubes (300 µl per tube). For subsequent RNA extraction, 600 µl Trizol Reagent (Invitrogen, 15-596-018) was added to each polyribosome fraction (300 µl), and samples were stored at -80 ^{o}C. RNA was extracted by adding 200 µl chloroform (Fisher, C298) to each fraction and centrifuging at 18,213 x g for 15 min. The aqueous phase was transferred to a tube containing 500 µl of isopropanol (Fisher, A416P-4) and 5 µg of glycogen (Sigma, G1767-1VL). Then samples were pelleted at 18,213 x g for 15 min, dried, washed with 70% ethanol, and centrifuged at 18,213 x g for 15 min. The pellet was dried and resuspended in 20 µl of Ultrapure water. Samples were digested with DNase (Roche) for 40 min at 37 ^{o}C. cDNA was generated using 2 µg of RNA for each fraction with a High-Capacity cDNA Reverse Transcription Kit (ThermoFisher, 4368814). qPCR was performed using PowerUp SYBR Green Master Mix (ThermoFisher, A25776) using a QuantStudio 5 Real-Time PCR System. Primers sequences were as follows: human Actin-F, TCCGTGTGGATCGGCGGCTCCA; human Actin-R, CTGCTTGCTGATCCACATCTG; human GRN-F, AGGAGAACGCTACCACGGA; and human GRN-R, GGCAGCAGGTATAGCCATCTG. Relative RNA levels were calculated using a C_t mean value normalized with an internal control (Actin). The delta C_T value is then normalized to the delta C_T value of the input (taken before the polyribosome profiling) from the corresponding condition.

AHA labeling. H4 cells were cultured in DMEM high glucose (Gibco, 11965-092) supplemented with 10% FBS (Gibco, 10010-023). Cells were cultured in 60-mm plate until about 80% confluence and treated with 10 µM ASOs for a total of 24 h. For optimal incorporation of the amino acid azidohomoalanine (AHA), cells were methionine-deprived for 2.5 h in methionine-free medium (DMEM without methionine, glutamine, and cysteine (Gibco, 21013024), supplemented with 0.5% FBS, 1X GlutaMAX (Gibco, 35050061), and 63 µg/ml L-Cysteine) containing 10 µM ASO. AHA was then added to the cell culture medium at a final concentration of 50 µM for the last 2 h of treatment to label de novo proteins. Cells were washed once with ice-cold PBS containing 0.1 mg/ml CHX, and then lysed in Triton lysis buffer containing 1% Triton X-100, 25 mM sodium pyrophosphate, 150 mM NaCl, 50 mM NaF, 5 mM EDTA, 5mM EGTA, 0.5% sodium deoxycholate, 20 mM HEPES pH 7.4, 10 mM β-glycerophosphate, 1 mM Na_3VO_4, 0.1 mg/ml CHX, and protease inhibitors (Roche, cOmplete Mini EDTA-free Protease Inhibitor Cocktail). Lysates were centrifuged (16,260 x g, 10 min, 4 °C), and the supernatant fractions were collected. Click reactions were performed using Click-iT Protein Reaction Buffer Kit (Invitrogen, C10276) according to the manufacturer's protocol in order to label the AHA-incorporated proteins with biotin alkyne (ThermoFisher, B10185). The Click reaction samples were incubated on a rotator at 4 °C for 1 h, and diluted in lysis buffer at a 1:2 ratio before being subjected to anti-progranulin immunoprecipitation. For immunoprecipitation, the lysates were incubated with rotation with 8.4 µg of anti-human progranulin linker 4 polyclonal antibody #611 (which recognizes an epitope between amino acids 422–440) (38) overnight at 4 °C, followed by a 2 h incubation with Protein A Agarose beads (Roche, 11719408001) at 4 °C. Beads were

washed three times with the lysis buffer and the immunoprecipitates were eluted, denatured and boiled (5 min, 95 °C) in 2X Laemmli buffer. For western blot analysis, the immunoprecipitated samples were resolved on 10% SDS–PAGE gels, transferred to nitrocellulose membranes, and stained with Ponceau. After blocking incubations, the membranes were incubated with IRDye 800CW Streptavidin (LICOR, 926-32230) to detect AHA-labelled proteins with the LICOR Odyssey imaging system. The membrane was reprobed with anti-human progranulin linker 5 polyclonal antibody #614 (1:3000) using Quick Western Kit-IRDye 680RD secondary antibody (LICOR, PN 926-69100).

MTT assay. MTT assays were used to assess the effects of ASOs on cell viability. H4 cells were plated in 96-well plates at a density of 5,000 cells per well. The following day, cell were treated with 10 µM ASO. After 21 h treatment, the media was removed and cells were incubated in 100 µl of 0.5 mg/ml thiazolyl blue tetrazolium bromide (MTT) (Sigma, M5655) solution prepared in fresh culture media for 4 h. After incubation, the MTT solution was removed and 100 µl of DMSO was added to dissolve the crystals formed. The absorbance was measured at 570 nm using a BioTek Synergy H1 plate reader. Experiments were performed with triplicate wells, and the percent viability was normalized to cells treated with vehicle only (water).

FRET-based assay for miR-29b binding. A FRET-based assay was developed to monitor the interaction between miR-29b (labeled with Cy3 at the 5' end) and a partial *GRN* 3' UTR RNA (nucleotides 189–246, labeled with Cy5 at the 3' end). Reactions were set up in duplicate wells in black 384-well plates with 1 µM miR-29b and 1 µM *GRN* 3' UTR in 20 µl of 1X SSC buffer, pH 7.0 containing 0.005% Tween-20. ASOs were added to the reactions in the same buffer at final concentrations between 0.64 nM–50 µM. Plates were read using a BioTek Synergy H1 plate reader with excitation at 540 nm and emission at 570 nm, and with excitation at 540 nm and emission at 665 nm. The ratio of fluorescence emissions at 665 nm / 570 nm was calculated for each well, and data were transformed with baseline correction.

Mouse studies. Animal procedures were approved by the Institutional Animal Care and Use Committee of Saint Louis University and followed NIH guidelines. Mice were housed in a pathogen-free barrier facility with a 12-h light/12-h dark cycle and provided food and water ad libitum. Humanized *GRN* mice (31) were on the C57BL/6J background and were genotyped either by PCR as described (31) or by real-time PCR (Transnetyx). Grn^{R493X} knockin mice (33) were on the C57BL/6J background and were genotyped by real-time PCR (Transnetyx). For ICV ASO delivery, 500 µg ASO (in 5 µl PBS) was administered by intracerebroventricular (ICV) bolus injection into the right lateral ventricle of mice anesthetized with isoflurane, as previously described (39). After 3 weeks, mice were sacrificed and brain tissues were collected for protein and RNA analyses. For ELISA, progranulin levels were determined in duplicate using 150 µg of protein lysates per well using a sandwich ELISA assay (abcam, ab252364). Western blot and qPCR analyses were carried out as described above. For immunofluorescence, mice were transcardially perfused with PBS followed by 4% paraformaldehyde; then 40-µm brain sections were stained using a previously described pan-ASO antibody that recognizes the ASO backbone (40). For IP ASO delivery, 50 mg/kg of ASO was administered every other day for a total of 4 injections. One day after the final injection, mice were sacrificed and tissues were collected for qPCR analysis.

Statistical analyses. Data are presented as means ± SD or as means ± SEM, as indicated in the figure legends. Data were analyzed with GraphPad Prism software using the statistical tests described in the figure legends. P values < 0.05 were considered significant.

Data Availability

The RNA-seq data used in this study are available in the Gene Expression Omnibus (GEO; http://www.ncbi.nlm.nih.gov/geo/) under accession code GSE188498. All the other data supporting the findings of this study are available within the article and its Supplementary Information files.

Acknowledgements

We thank Michael Ward for providing iPSCs for differentiation into i3 neurons, the Genomics Core Facility at Saint Louis University for RNA-seq, Sophie Chang for technical assistance, and Laura Mitic and Robert Farese, Jr. for helpful discussions. This work was supported by grants from the NIH (AG064069), NIH/National Center for Advancing Translational Sciences (NCATS) (UL1TR002345), Bluefield Project to Cure FTD, Natural Sciences and Engineering Research Council of Canada (NSERC, RGPIN-2018-06227, RGPIN-2020-06376, DGECR-2018-00093, and DGECR-2020-00060), Brain Canada Future Leaders Grant, and Fonds de Recherche du Québec Santé Junior-1.

References

1. A. W. Kao, A. McKay, P. P. Singh, A. Brunet, E. J. Huang, Progranulin, lysosomal regulation and neurodegenerative disease. *Nat. Rev. Neurosci.* **18**, 325-333 (2017).
2. D. H. Paushter, H. Du, T. Feng, F. Hu, The lysosomal function of progranulin, a guardian against neurodegeneration. *Acta Neuropathol.* **136**, 1-17 (2018).
3. M. Cruts *et al.*, Null mutations in progranulin cause ubiquitin-positive frontotemporal dementia linked to chromosome 17q21. *Nature* **442**, 920-924 (2006).
4. M. Baker *et al.*, Mutations in progranulin cause tau-negative frontotemporal dementia linked to chromosome 17. *Nature* **442**, 916-919 (2006).
5. J. Terryn, C. M. Verfaillie, P. Van Damme, Tweaking progranulin expression: therapeutic avenues and opportunities. *Front. Mol. Neurosci.* **14**, 713031 (2021).
6. S. Amin, G. Carling, L. Gan, New insights and therapeutic opportunities for progranulin-deficient frontotemporal dementia. *Curr. Opin. Neurobiol.* **72**, 131-139 (2021).
7. A. E. Arrant, A. J. Filiano, D. E. Unger, A. H. Young, E. D. Roberson, Restoring neuronal progranulin reverses deficits in a mouse model of frontotemporal dementia. *Brain* **140**, 1447-1465 (2017).
8. B. Cenik *et al.*, Suberoylanilide hydroxamic acid (vorinostat) up-regulates progranulin transcription: rational therapeutic approach to frontotemporal dementia. *J. Biol. Chem.* **286**, 16101-16108 (2011).

9. C. J. Holler *et al.*, Trehalose upregulates progranulin expression in human and mouse models of GRN haploinsufficiency: a novel therapeutic lead to treat frontotemporal dementia. *Mol. Neurodegener.* **11**, 46 (2016).
10. S. J. Sha *et al.*, An 8-week, open-label, dose-finding study of nimodipine for the treatment of progranulin insufficiency from GRN gene mutations. *Alzheimers Dement (N Y)* **3**, 507-512 (2017).
11. P. A. Ljubenkov *et al.*, Effect of the histone deacetylase inhibitor FRM-0334 on progranulin levels in patients with progranulin gene haploinsufficiency: a randomized clinical trial. *JAMA Netw Open* **4**, e2125584 (2021).
12. C. Hinderer *et al.*, Adeno-associated virus serotype 1-based gene therapy for FTD caused by GRN mutations. *Ann Clin Transl Neurol* **7**, 1843-1853 (2020).
13. Alzforum (2021) AL001 boosts progranulin. Does it slow frontotemporal dementia?
14. T. Logan *et al.*, Rescue of a lysosomal storage disorder caused by Grn loss of function with a brain penetrant progranulin biologic. *Cell* **184**, 4651-4668.e4625 (2021).
15. K. M. Schoch, T. M. Miller, Antisense oligonucleotides: Translation from mouse models to human neurodegenerative diseases. *Neuron* **94**, 1056-1070 (2017).
16. B. R. Leavitt, S. J. Tabrizi, Antisense oligonucleotides for neurodegeneration. *Science* **367**, 1428-1429 (2020).
17. X. H. Liang *et al.*, Translation efficiency of mRNAs is increased by antisense oligonucleotides targeting upstream open reading frames. *Nat. Biotechnol.* **34**, 875-880 (2016).
18. X. H. Liang *et al.*, Antisense oligonucleotides targeting translation inhibitory elements in 5' UTRs can selectively increase protein levels. *Nucleic Acids Res.* **45**, 9528-9546 (2017).
19. R. C. Friedman, K. K. Farh, C. B. Burge, D. P. Bartel, Most mammalian mRNAs are conserved targets of microRNAs. *Genome Res.* **19**, 92-105 (2009).
20. H. O. Iwakawa, Y. Tomari, The functions of microRNAs: mRNA decay and translational repression. *Trends Cell Biol.* **25**, 651-665 (2015).
21. J. O'Brien, H. Hayder, Y. Zayed, C. Peng, Overview of microRNA biogenesis, mechanisms of actions, and circulation. *Front Endocrinol* **9**, 402 (2018).
22. J. Jiao, L. D. Herl, R. V. Farese, F. B. Gao, MicroRNA-29b regulates the expression level of human progranulin, a secreted glycoprotein implicated in frontotemporal dementia. *PLoS One* **5**, e10551 (2010).
23. L. Chen *et al.*, MiR-29b-3p promotes chondrocyte apoptosis and facilitates the occurrence and development of osteoarthritis by targeting PGRN. *J. Cell. Mol. Med.* **21**, 3347-3359 (2017).
24. R. Rademakers *et al.*, Common variation in the miR-659 binding-site of GRN is a major risk factor for TDP43-positive frontotemporal dementia. *Hum. Mol. Genet.* **17**, 3631-3642 (2008).
25. P. Piscopo *et al.*, Reduced miR-659-3p levels correlate with progranulin increase in hypoxic conditions: implications for frontotemporal dementia. *Front. Mol. Neurosci.* **9**, 31 (2016).
26. W. X. Wang *et al.*, miR-107 regulates granulin/progranulin with implications for traumatic brain injury and neurodegenerative disease. *Am. J. Pathol.* **177**, 334-345 (2010).
27. J. Sheng, L. Su, Z. Xu, G. Chen, Progranulin polymorphism rs5848 is associated with increased risk of Alzheimer's disease. *Gene* **542**, 141-145 (2014).
28. M. J. Lee, T. F. Chen, T. W. Cheng, M. J. Chiu, rs5848 variant of progranulin gene is a risk of Alzheimer's disease in the Taiwanese population. *Neurodegener. Dis.* **8**, 216-220 (2011).
29. L. H. Meeter *et al.*, Progranulin levels in plasma and cerebrospinal fluid in granulin mutation carriers. *Dement Geriatr Cogn Dis Extra* **6**, 330-340 (2016).
30. N. Ludwig *et al.*, Distribution of miRNA expression across human tissues. *Nucleic Acids Res.* **44**, 3865-3877 (2016).
31. T. L. Petkau *et al.*, Human progranulin-expressing mice as a novel tool for the development of progranulin-modulating therapeutics. *Neurobiol. Dis.* **153**, 105314 (2021).

32. P. Jafar-Nejad *et al.*, The atlas of RNase H antisense oligonucleotide distribution and activity in the CNS of rodents and non-human primates following central administration. *Nucleic Acids Res.* **49**, 657-673 (2021).
33. A. D. Nguyen *et al.*, Murine knockin model for progranulin-deficient frontotemporal dementia with nonsense-mediated mRNA decay. *Proc. Natl. Acad. Sci. U. S. A.* **115**, E2849-E2858 (2018).
34. W. Y. Choi, A. J. Giraldez, A. F. Schier, Target protectors reveal dampening and balancing of Nodal agonist and antagonist by miR-430. *Science* **318**, 271-274 (2007).
35. V. Viart *et al.*, Transcription factors and miRNAs that regulate fetal to adult CFTR expression change are new targets for cystic fibrosis. *Eur. Respir. J.* **45**, 116-128 (2015).
36. M. Cruts, J. Theuns, C. Van Broeckhoven, Locus-specific mutation databases for neurodegenerative brain diseases. *Hum. Mutat.* **33**, 1340-1344 (2012).
37. M. S. Fernandopulle *et al.*, Transcription factor-mediated differentiation of human iPSCs into neurons. *Curr. Protoc. Cell Biol.* **79**, e51 (2018).
38. A. D. Nguyen *et al.*, Secreted progranulin is a homodimer and is not a component of high density lipoproteins (HDL). *J. Biol. Chem.* **288**, 8627-8635 (2013).
39. S. A. Farr, M. A. Erickson, M. L. Niehoff, W. A. Banks, J. E. Morley, Central and peripheral administration of antisense oligonucleotide targeting amyloid-β protein precursor improves learning and memory and reduces neuroinflammatory cytokines in Tg2576 (AβPPswe) mice. *J. Alzheimers Dis.* **40**, 1005-1016 (2014).
40. S. L. DeVos *et al.*, Tau reduction prevents neuronal loss and reverses pathological tau deposition and seeding in mice with tauopathy. *Sci. Transl. Med.* **9**, eaag0481 (2017).

FIGURE LEGENDS

Fig. 1. Inhibition of miR-29b increases progranulin protein levels. (A) ELISA for progranulin protein levels in H4 neuroglioma cells following treatment with miR-29b inhibitor for 24 h. (B) miR-29b is moderately expressed in human H4 neuroglioma cells. Ranked profile of miR expression levels, as determined by RNA-seq. miR-29b is indicated in red. (C) Expression levels of miRs known to regulate progranulin levels in the human brain. Data from the Human miRNA Tissue Atlas (30). Data are presented as means ± SD; ** indicates $p<0.01$, as determined by one-way ANOVA with Dunnett post hoc test.

Fig. 2. ASOs targeting the miR-29 binding site in the human *GRN* mRNA increase progranulin protein levels. (A) Schematic of the *GRN* 3' UTR indicating miR binding sites and region targeted by ASOs. (B) Validation of ASO hits from initial screening. H4 cells were treated with 5 µM ASO for 24 h, and progranulin levels were measured in cell lysates by ELISA. (C) Western blot validation of candidate ASOs in H4 cells (10 µM, 24 h). (D) ASOs increase both cellular and secreted progranulin levels. After treatment with 10 µM ASO for 24 h, progranulin levels in cell lysates and in the conditioned media were determined by western blot. Data are presented as means ± SD; * indicates $p<0.05$, ** indicates $p<0.01$, *** indicates $p<0.001$, **** indicates $p<0.0001$, as determined by one-way ANOVA with Dunnett post hoc test.

Fig. 3. Time course and dose curve experiments for selected ASOs. (A) ASOs increase progranulin protein levels within several hours. H4 cells were treated with 10 µM ASO for the indicated times, and progranulin levels in cell lysates were determined by western blot. (B) Dose

curve of ASO treatment in H4 cells (24 h). Progranulin levels were measured in cell lysates by ELISA. Data are presented as means ± SD, with EC_{50} values indicated.

Fig. 4. ASOs increase progranulin protein levels in iPSC-derived neurons and in mouse brains. (A) Western blot of progranulin in iPSC-derived neurons following ASO treatment at the indicated concentrations (µM) for 3–4 days. (B-C) Human progranulin levels in brains of humanized *GRN* mice at 3 weeks after ICV administration of 500 µg ASO. (B) Human progranulin levels in cortex, as determined by ELISA. (C) Western blot of human progranulin in cortex, thalamus, and hippocampus. Data are presented as means ± SEM; * indicates $p<0.05$, as determined by one-way ANOVA with Dunnett post hoc test. Non-Tg, non-transgenic.

Fig. 5. ASOs increase progranulin translation. (A) *GRN* mRNA levels following ASO treatment (5 µM, 24 h), as determined by qPCR. (B) *GRN* mRNA distribution in each of 16 sucrose gradient fractions from ASO-treated H4 cells (5 µM, 22 h) analyzed by qPCR. Fraction 1: hydrosoluble fraction; fractions 2, 3, and 4: 40S, 60S, and monosomes, respectively; fractions 5–10: light polyribosomes; and fractions 11–16: heavy polyribosomes. Data are plotted as a fraction of total mRNA on the gradient. (C) Western blot showing immunoprecipated, newly synthesized, AHA/biotin-labeled progranulin protein following ASO treatment (10 µM, 24 h). Data are presented as means ± SD; * indicates $p<0.05$ and ** indicates $p<0.01$, as determined by one-way ANOVA with Dunnett post hoc test. PGRN, progranulin.

Fig. 6. ASOs act through blocking miR-29b binding. (A) ASOs require miR-29b to increase progranulin protein levels. ELISA for progranulin protein levels after co-treatment with miR-29b inhibitor (70 µM) and ASOs (20 µM) for 24 h. (B) FRET assay demonstrating multiple ASOs can compete miR-29b from binding to a partial *GRN* 3' UTR RNA. Data are presented as means ± SD; ** indicates $p<0.01$ and *** indicates $p<0.001$ as determined by two-way ANOVA with Tukey post hoc test. n.s., not significant.

SUPPLEMENTAL FIGURE LEGENDS

Fig. S1. ASOs are not toxic in cells. H4 cells were treated with 10 µM ASO for 21 h, and then cell viability was assessed by MTT assay. Data are presented as means ± SD.

Fig. S2. ICV administration of ASOs targeting NMD of the Grn^{R493X} mRNA does not increase *Grn* mRNA levels in the brains of $Grn^{R493X/R493X}$ mice. qPCR results from brains of $Grn^{R493X/R493X}$ mice at 2–3 weeks after ICV administration of 200–500 µg ASO. (A) *Grn* mRNA levels are presented relative to levels in tissues of wild-type mice that received control ASO. (B) *Malat1* mRNA levels in wild-type mice. Data are presented as means ± SEM; * indicates $p<0.05$ and ** indicates $p<0.01$, as determined by one-way ANOVA with Dunnett post hoc test in (A) and by t-test in (B). n.s., not significant.

Fig. S3. ICV administration of ASOs targeting NMD of the Grn^{R493X} mRNA does not increase brain progranulin protein levels. Western blot of mouse progranulin levels in cortex of $Grn^{R493X/R493X}$ mice at 2 weeks after ICV administration of 500 µg ASO.

Fig. S4. ASOs are distributed throughout the brain. At 3 weeks after ICV administration of saline or NMD-targeting *Grn* ASO B (200 µg), brains were fixed and sections were stained with an ASO-antibody (red) and counterstained with nuclear stain DAPI (blue).

Fig. S5. IP administration of ASOs targeting NMD of the Grn^{R493X} mRNA does not increase *Grn* mRNA levels in the livers and spleens. qPCR results from livers and spleens of $Grn^{R493X/R493X}$ mice following a series of four IP administrations of 50 mg/kg ASO. (A) *Grn* mRNA levels are presented relative to levels in tissues of wild-type mice that received control ASO. (B) *Malat1* mRNA levels in wild-type mice. Data are presented as means ± SEM; * indicates $p<0.05$, as determined by one-way ANOVA with Dunnett post hoc test in (A) and by t-test in (B). n.s., not significant.

Fig. S6. ASOs targeting NMD of the Grn^{R493X} mRNA increase *Grn* mRNA levels in $Grn^{R493X/R493X}$ MEF cells. Cells were transfected with 100 nM ASO using Lipofectamine 2000. After 24 hours, RNA was isolated for qPCR. Data are presented as means ± SD; * indicates $p<0.05$, ** indicates $p<0.01$, *** indicates $p<0.001$, **** indicates $p<0.0001$, as determined by one-way ANOVA with Dunnett post hoc test.

Fig. S7. Several ASOs targeting the miR-659 binding site in the *GRN* 3' UTR increase progranulin protein levels. H4 cells were treated with 5 µM ASO for 24 h, and progranulin levels were measured in cell lysates by ELISA. Data are presented as means ± SD; * indicates $p<0.05$ and ** indicates $p<0.01$, as determined by one-way ANOVA with Dunnett post hoc test.

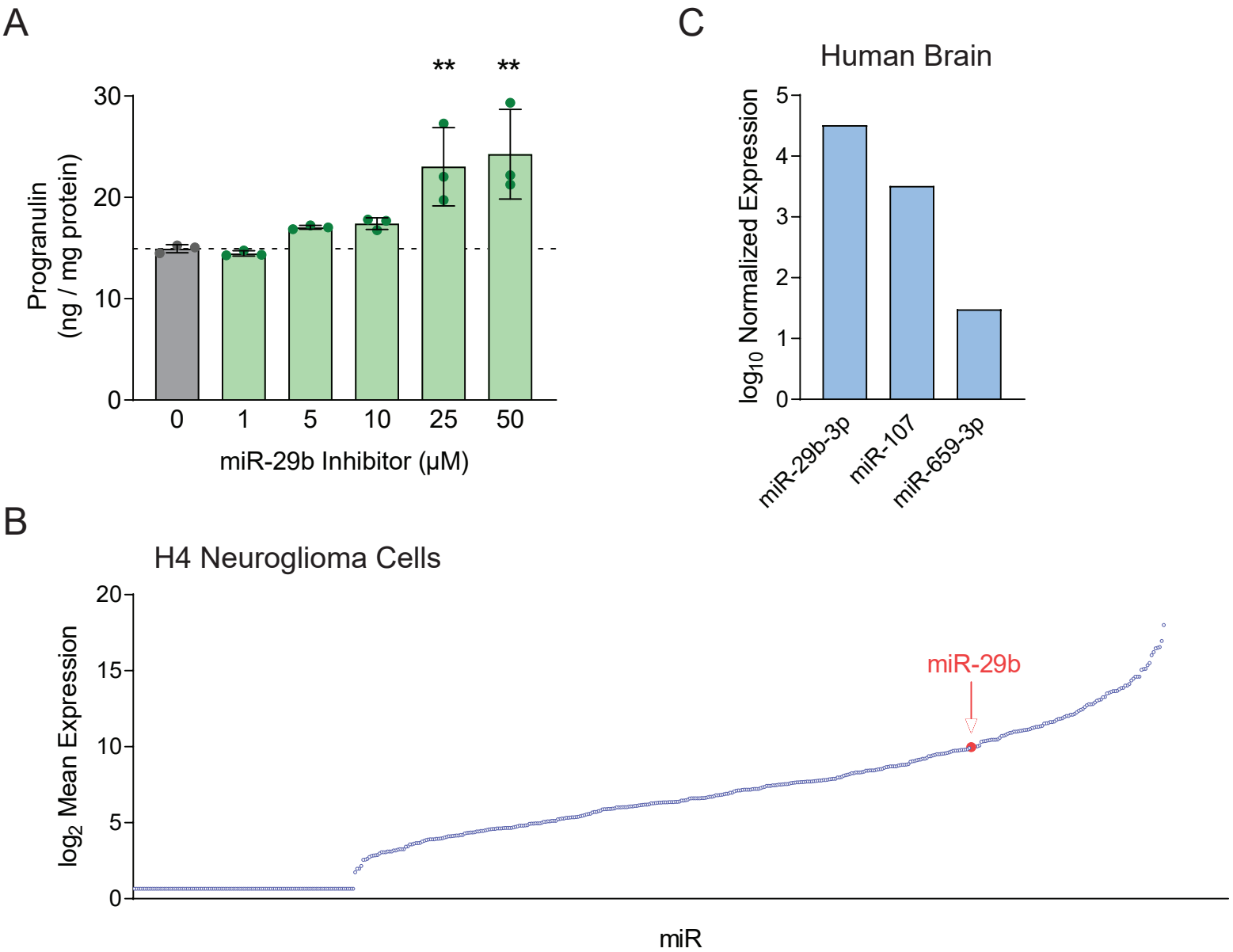
A
**
**
30
20
10
0
Progranulin
(ng / mg protein)
0
1
5
10
25
50
miR-29b Inhibitor (μM)
C
Human Brain
5
4
3
2
1
0
log10 Normalized Expression
miR-29b-3p
miR-107
miR-659-3p
B
H4 Neuroglioma Cells
20
15
10
5
0
log2 Mean Expression
miR-29b
miR

Figure 1

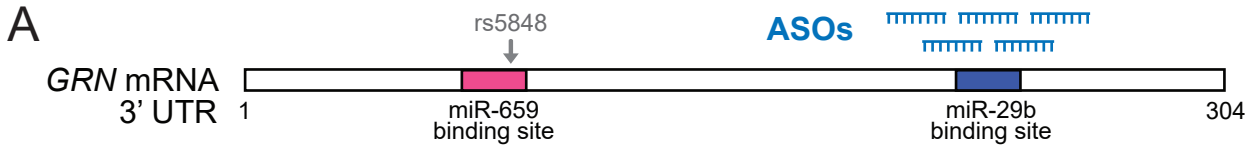
A
rs5848
ASOs
GRN mRNA
3' UTR
1
miR-659
binding site
miR-29b
binding site
304

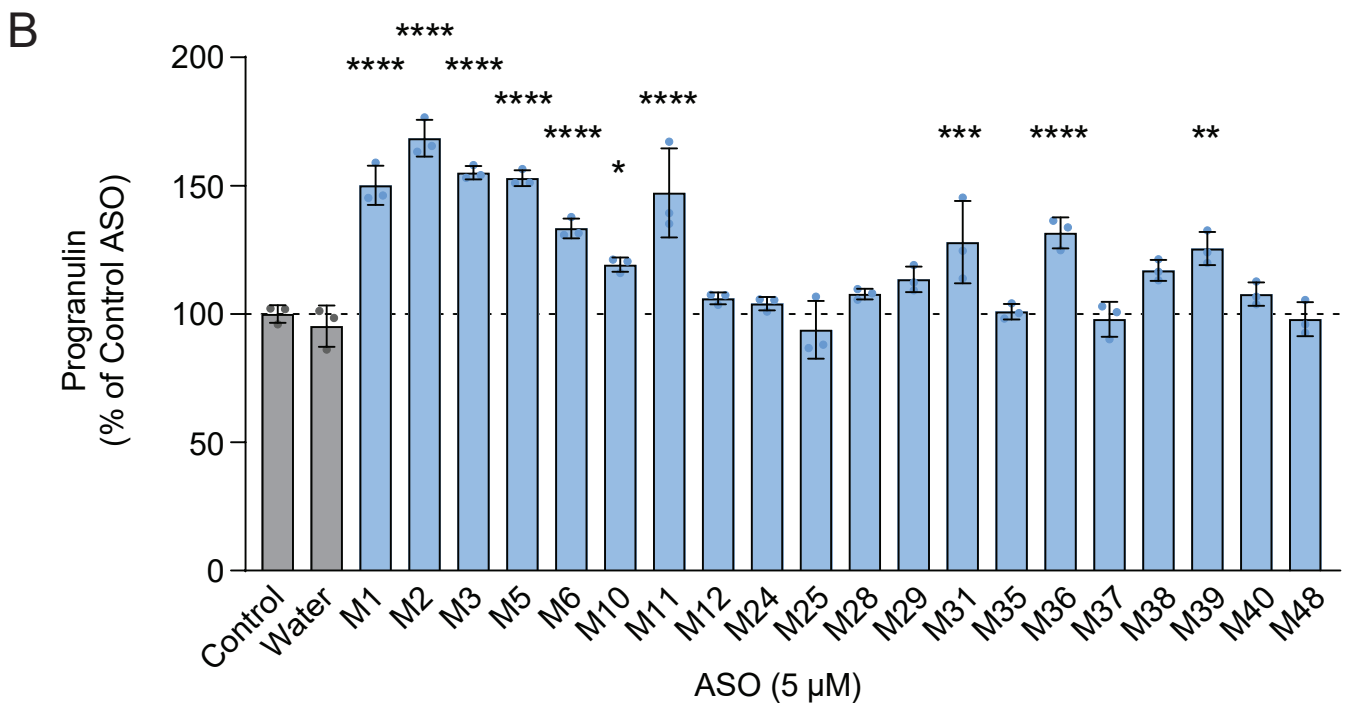
B
Progranulin
(% of Control ASO)
200
150
100
50
0
****
****
****
****
****
****
*
***
****
**
Control
Water
M1
M2
M3
M5
M6
M10
M11
M12
M24
M25
M28
M29
M31
M35
M36
M37
M38
M39
M40
M48
ASO (5 μM)

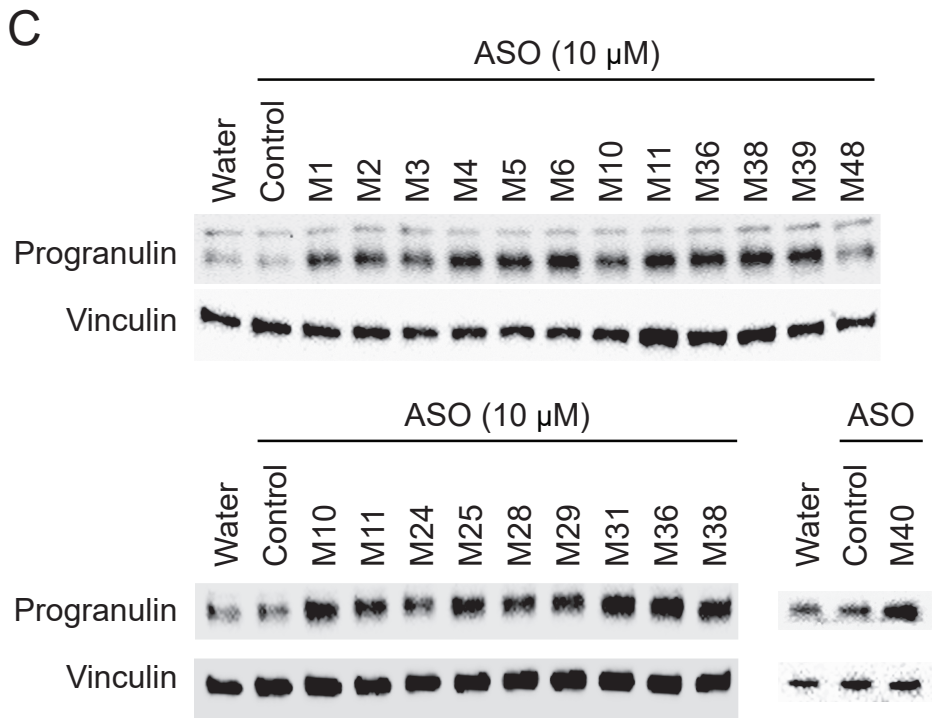
C
ASO (10 μM)
Water
Control
M1
M2
M3
M4
M5
M6
M10
M11
M36
M38
M39
M48
Progranulin
Vinculin
ASO (10 μM)
Water
Control
M10
M11
M24
M25
M28
M29
M31
M36
M38
Progranulin
Vinculin
ASO
Water
Control
M40

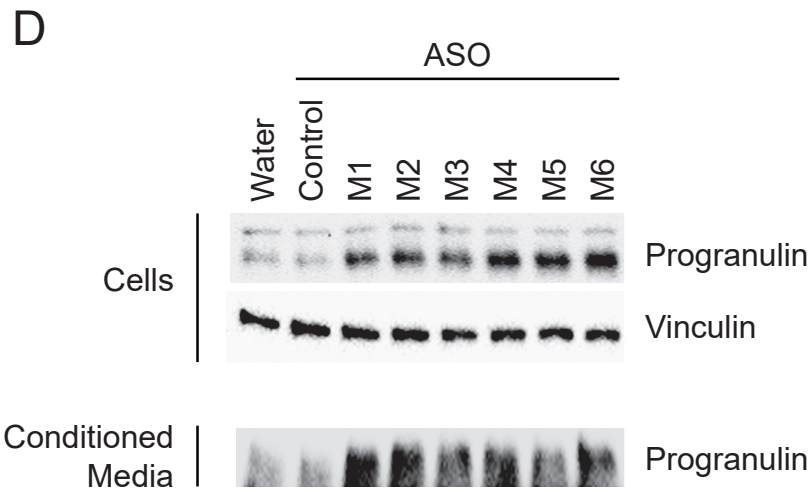
D
ASO
Water
Control
M1
M2
M3
M4
M5
M6
Cells
Progranulin
Vinculin
Conditioned
Media
Progranulin

Figure 2

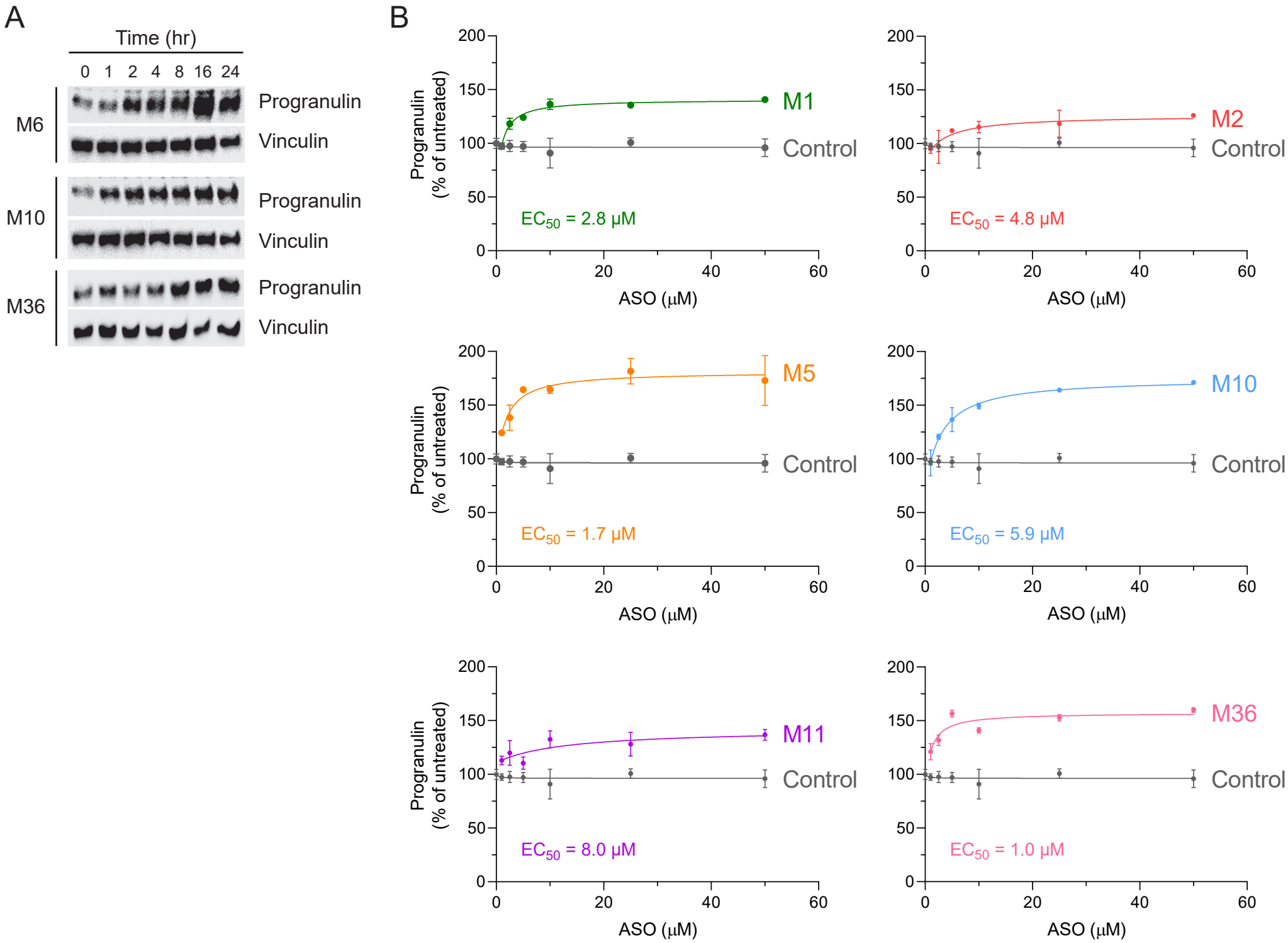
A
Time (hr)
0 1 2 4 8 16 24
M6
Progranulin
Vinculin
M10
Progranulin
Vinculin
M36
Progranulin
Vinculin
B
Progranulin (% of untreated)
ASO (μM)
M1
Control
EC50 = 2.8 μM
M2
Control
EC50 = 4.8 μM
M5
Control
EC50 = 1.7 μM
M10
Control
EC50 = 5.9 μM
M11
Control
EC50 = 8.0 μM
M36
Control
EC50 = 1.0 μM

Figure 3

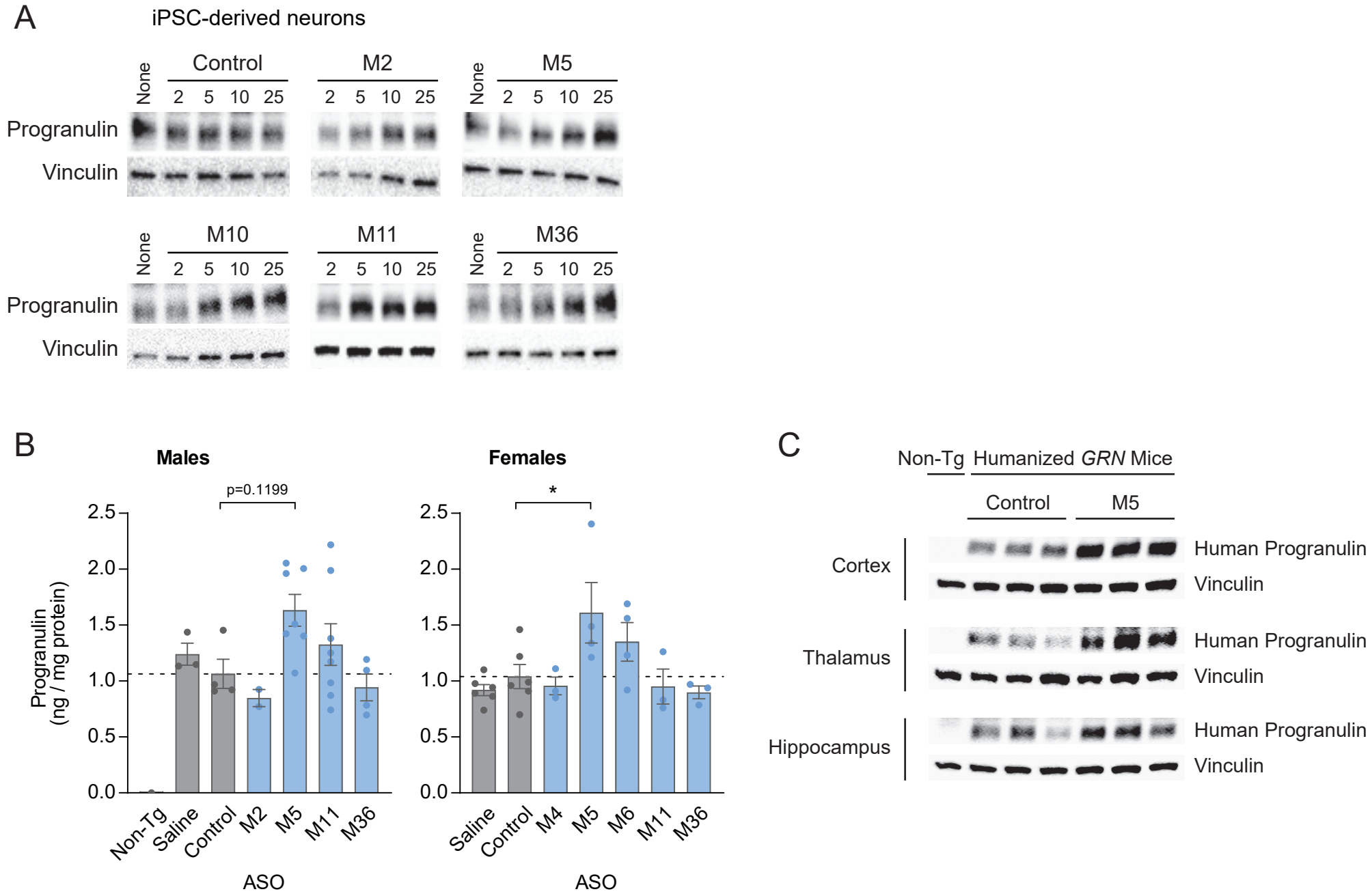
A
iPSC-derived neurons
Control
M2
M5
M10
M11
M36
None
2
5
10
25
Progranulin
Vinculin
B
Males
Females
p=0.1199
*
Progranulin
(ng / mg protein)
2.5
2.0
1.5
1.0
0.5
0.0
Non-Tg
Saline
Control
M2
M5
M11
M36
M4
M6
ASO
C
Non-Tg
Humanized GRN Mice
Control
M5
Cortex
Thalamus
Hippocampus
Human Progranulin
Vinculin

Figure 4

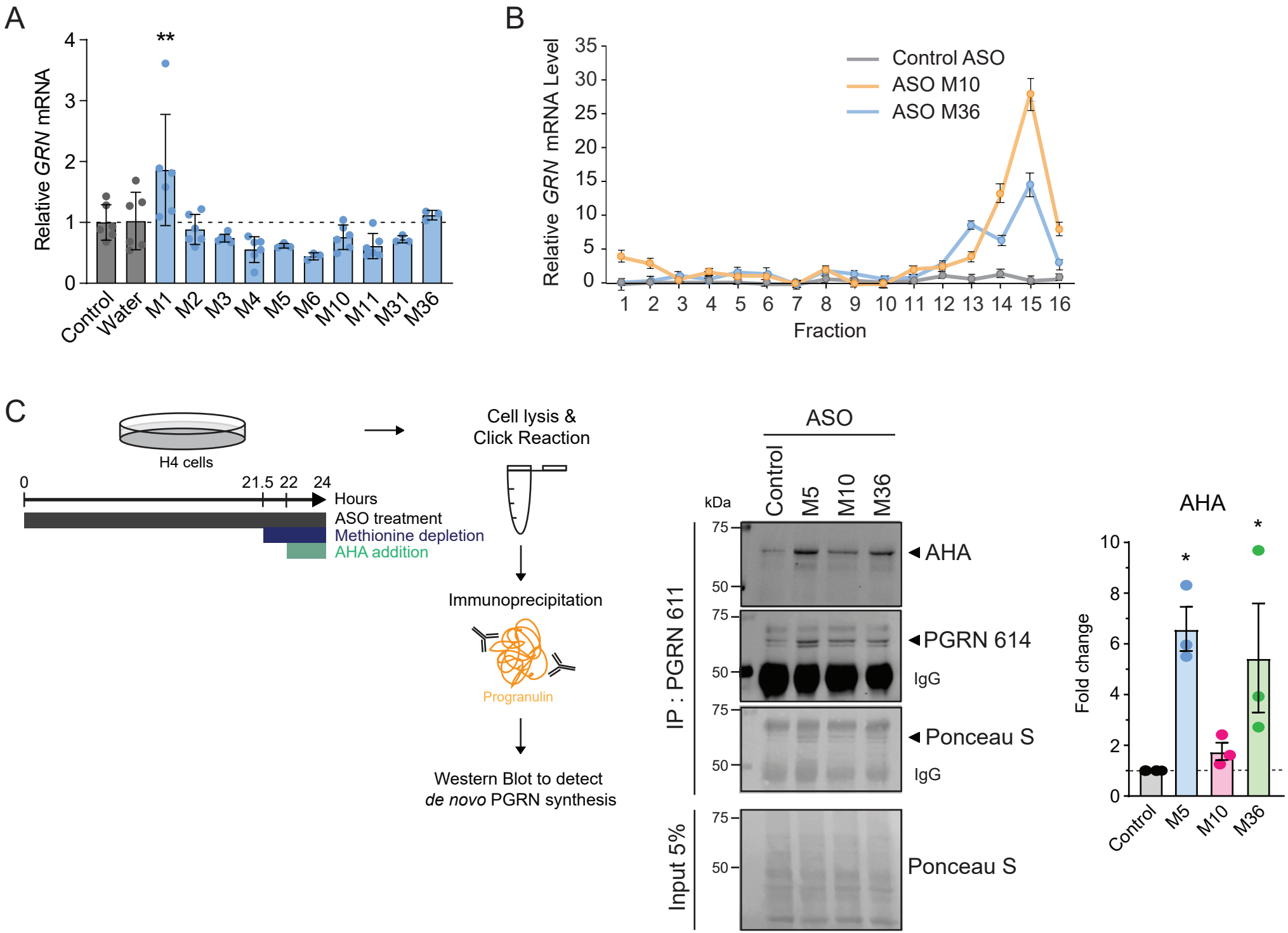
A
Relative GRN mRNA
**
Control
Water
M1
M2
M3
M4
M5
M6
M10
M11
M31
M36
B
Relative GRN mRNA Level
Control ASO
ASO M10
ASO M36
Fraction
C
H4 cells
0
21.5 22 24
Hours
ASO treatment
Methionine depletion
AHA addition
Cell lysis &
Click Reaction
Immunoprecipitation
Progranulin
Western Blot to detect
de novo PGRN synthesis
ASO
Control
M5
M10
M36
kDa
AHA
PGRN 614
IgG
Ponceau S
IgG
IP : PGRN 611
Input 5%
Ponceau S
AHA
Fold change
Control
M5
M10
M36

Figure 5

A

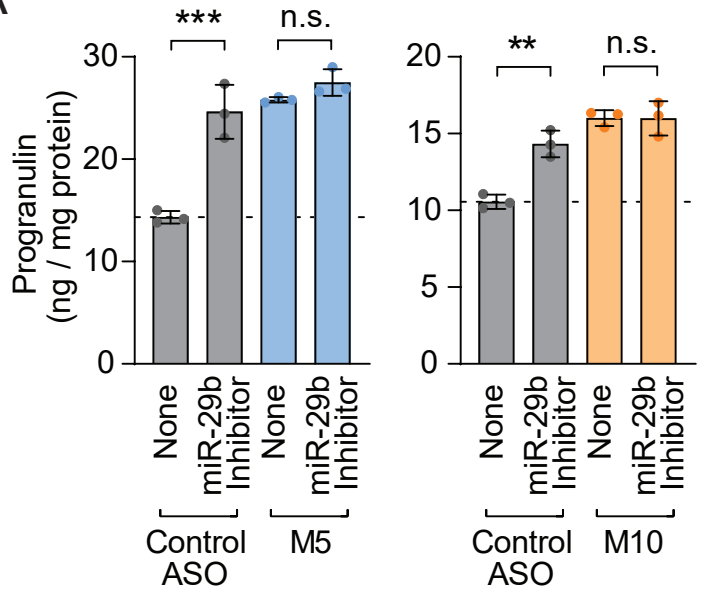
***
n.s.
**
n.s.
Progranulin
(ng / mg protein)
30
20
10
0
20
15
10
5
0
None
miR-29b Inhibitor
None
miR-29b Inhibitor
None
miR-29b Inhibitor
None
miR-29b Inhibitor
Control ASO
M5
Control ASO
M10

B

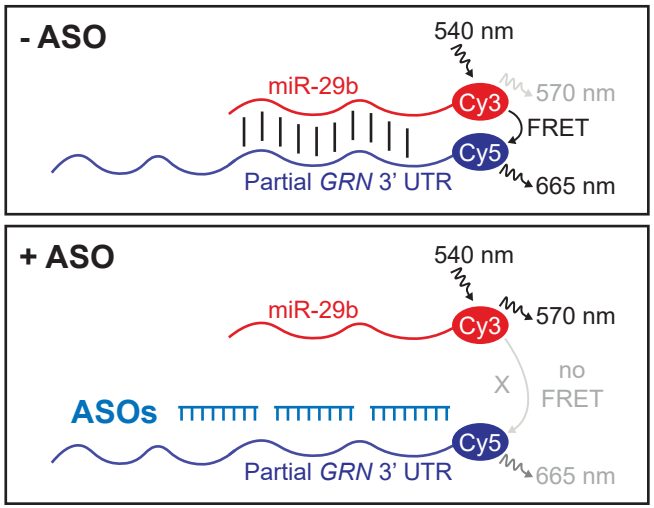
- ASO
540 nm
miR-29b
Cy3
570 nm
FRET
Cy5
665 nm
Partial GRN 3' UTR
+ ASO
540 nm
miR-29b
Cy3
570 nm
X
no FRET
ASOs
Cy5
665 nm
Partial GRN 3' UTR

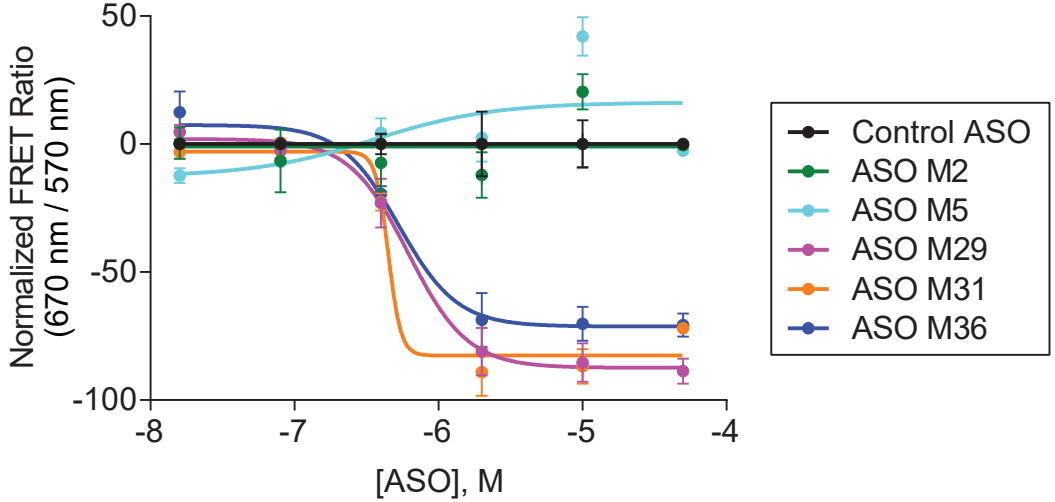
Normalized FRET Ratio
(670 nm / 570 nm)
50
0
-50
-100
-8
-7
-6
-5
-4
[ASO], M
Control ASO
ASO M2
ASO M5
ASO M29
ASO M31
ASO M36

Figure 6

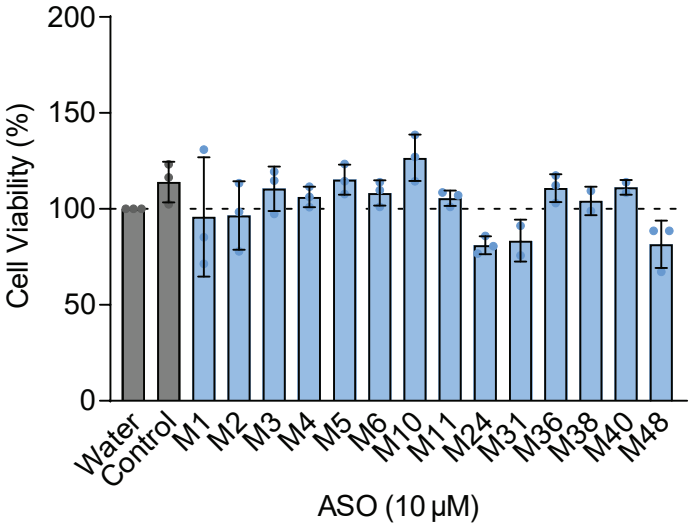
200
150
100
50
0
Cell Viability (%)
Water Control
M1
M2
M3
M4
M5
M6
M10
M11
M24
M31
M36
M38
M40
M48
ASO (10 μM)

Figure S1

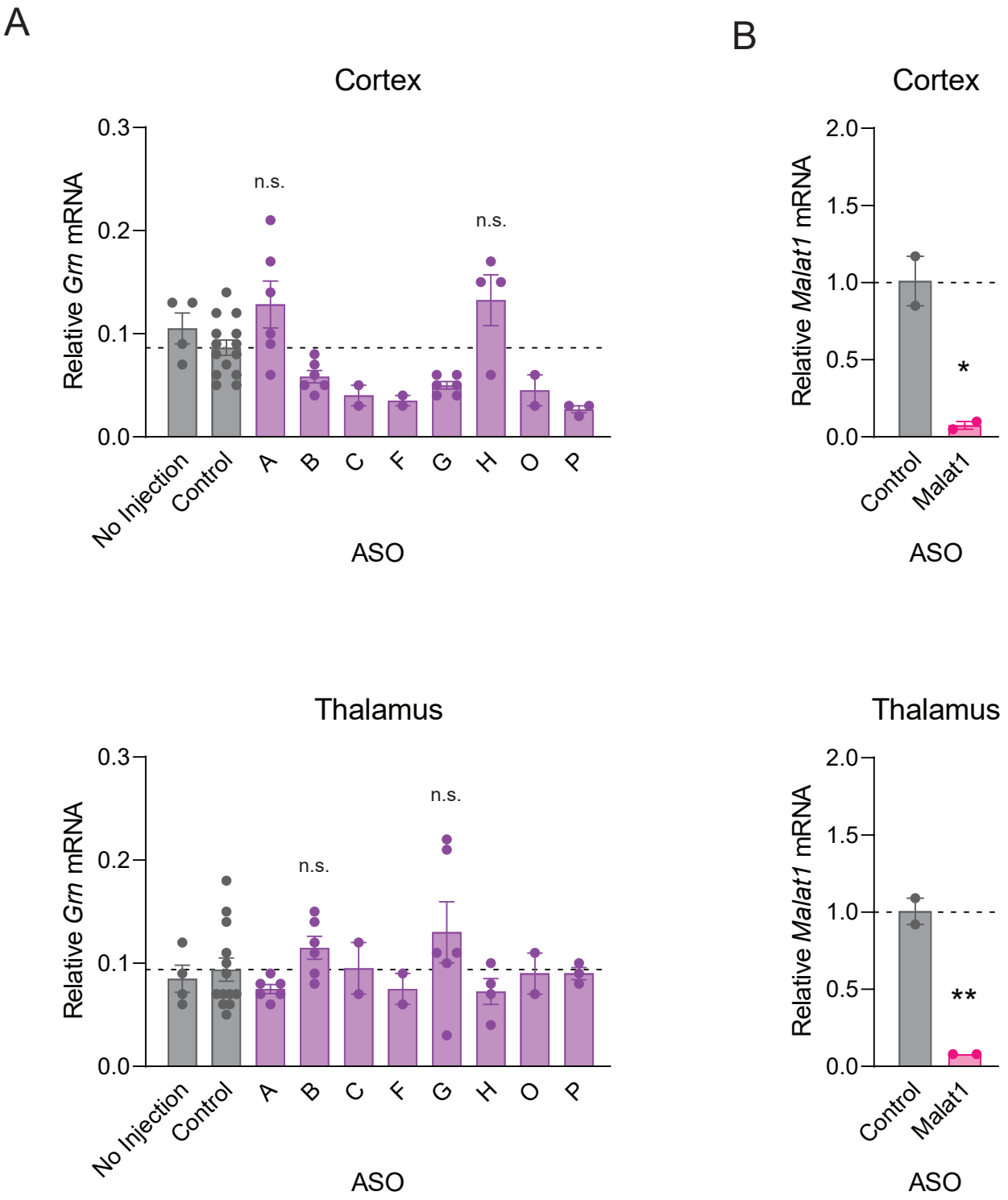
A
Cortex
Relative Grn mRNA
0.3
0.2
0.1
0.0
n.s.
n.s.
No Injection
Control
A
B
C
F
G
H
O
P
ASO
B
Cortex
Relative Malat1 mRNA
2.0
1.5
1.0
0.5
0.0
*
Control
Malat1
ASO
Thalamus
Relative Grn mRNA
0.3
0.2
0.1
0.0
n.s.
n.s.
No Injection
Control
A
B
C
F
G
H
O
P
ASO
Thalamus
Relative Malat1 mRNA
2.0
1.5
1.0
0.5
0.0
**
Control
Malat1
ASO

Figure S2

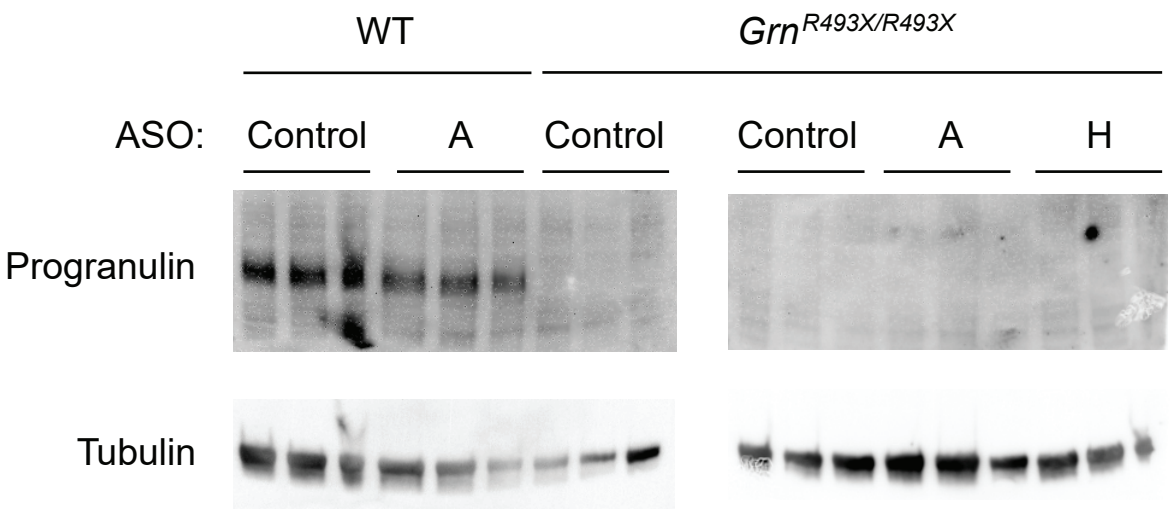
WT
Grn R493X/R493X
ASO:
Control
A
Control
Control
A
H
Progranulin
Tubulin

Figure S3

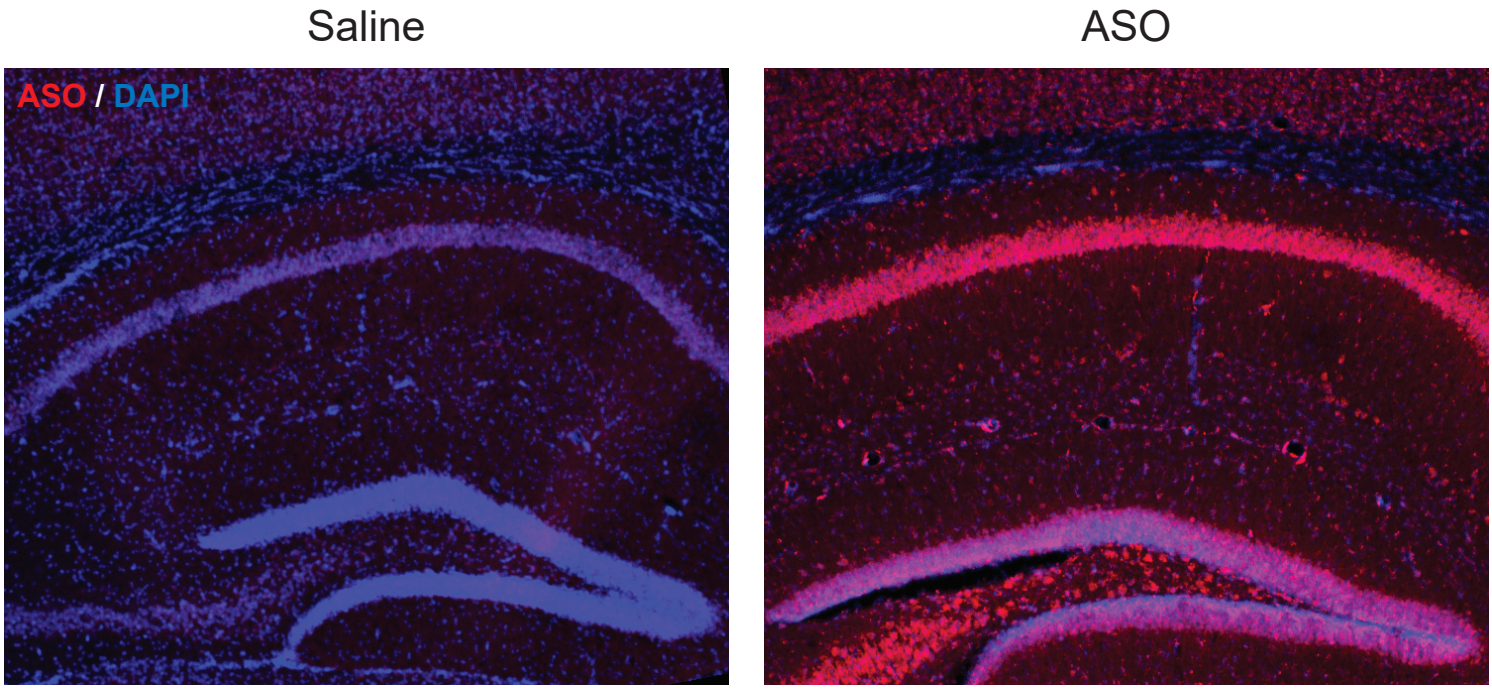

Figure S4

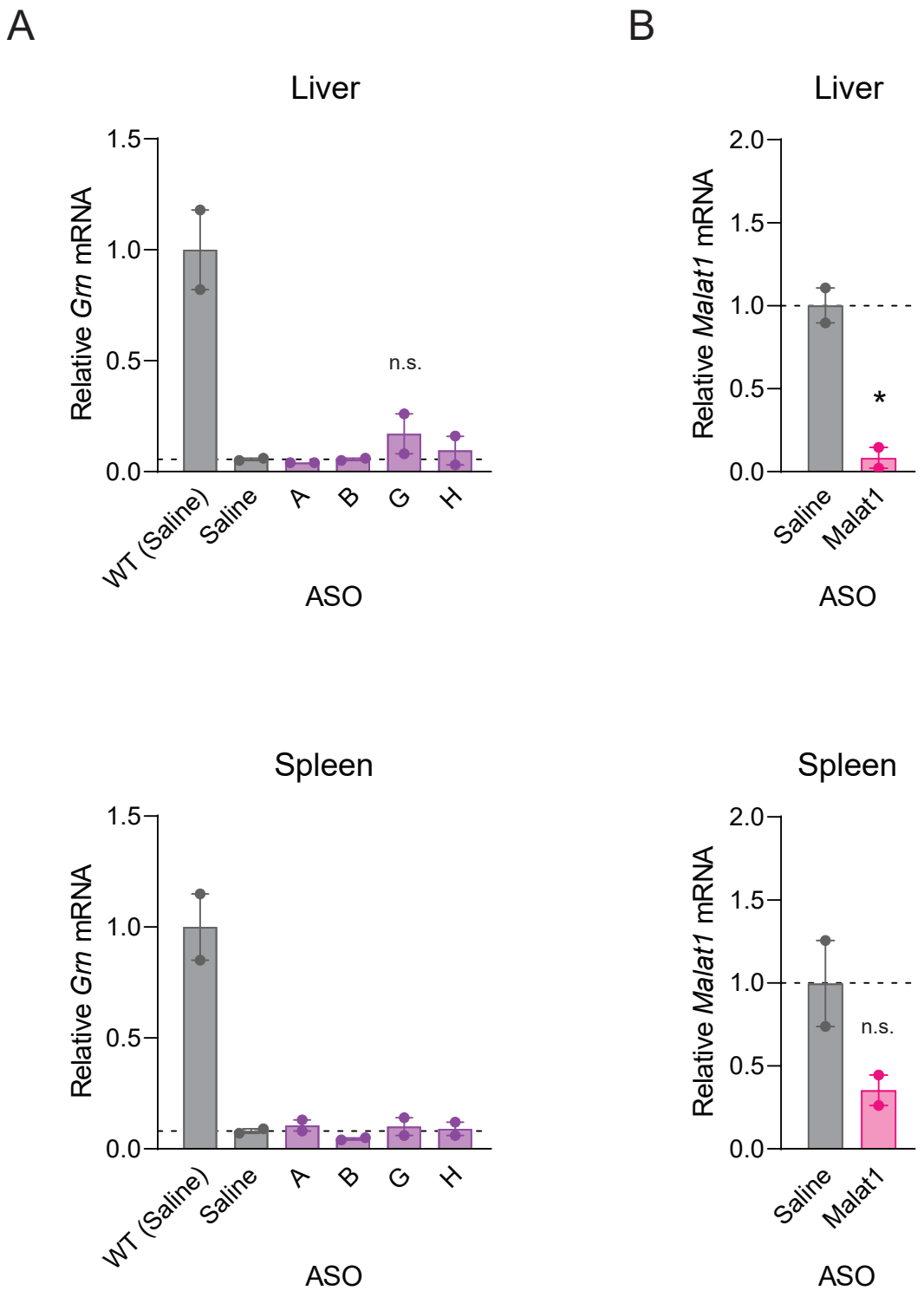
A
B
Liver
Relative Grn mRNA
1.5
1.0
0.5
0.0
n.s.
WT (Saline)
Saline
A
B
G
H
ASO
Liver
Relative Malat1 mRNA
2.0
1.5
1.0
0.5
0.0
*
Saline
Malat1
ASO
Spleen
Relative Grn mRNA
1.5
1.0
0.5
0.0
WT (Saline)
Saline
A
B
G
H
ASO
Spleen
Relative Malat1 mRNA
2.0
1.5
1.0
0.5
0.0
n.s.
Saline
Malat1
ASO

Figure S5

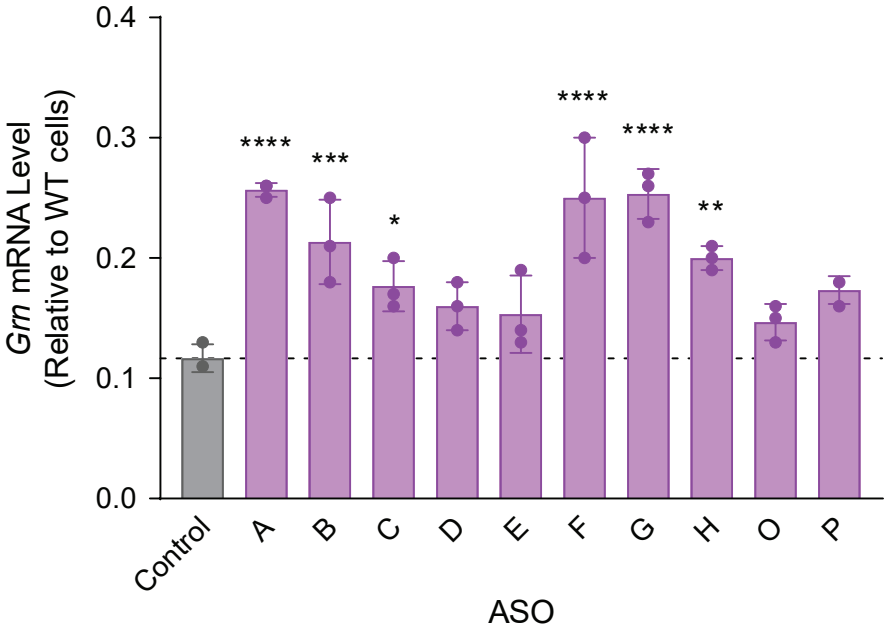
0.4
0.3
0.2
0.1
0.0
Grn mRNA Level
(Relative to WT cells)
****
***
*
****
****
**
Control
A
B
C
D
E
F
G
H
O
P
ASO

Figure S6

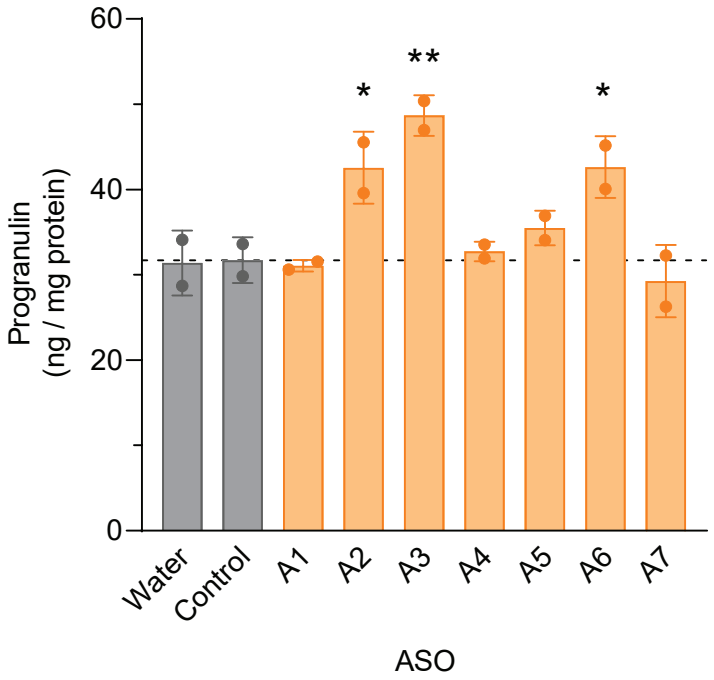
60
40
20
0
Progranulin
(ng / mg protein)
*
**
*
Water
Control
A1
A2
A3
A4
A5
A6
A7
ASO

Figure S7